Gap Junction Protein Expression in Hyperoxia-Exposed Neonatal Rat Lung Tissue

Cai Qing
Shengjing Hospital of China Medical University
Yu Xuefei
Shengjing Hospital of China Medical University
Xue Xindong
Shengjing Hospital of China Medical University
Fu Jianhua (fujianhua2021@163.com)
Shengjing Hospital of China Medical University

Research Article

Keywords: bronchopulmonary dysplasia, oxidative stress, apoptosis, connexins

Posted Date: September 21st, 2022

DOI: https://doi.org/10.21203/rs.3.rs-1979743/v1

Abstract

Bronchopulmonary dysplasia (BPD) is a common devastating pulmonary complication in preterm infants. Gap junction is involved in many lung diseases. In this study, we examine the expression of gap junction proteins, including connexin 26 (Cx26), connexin 32 (Cx32), connexin 43 (Cx43), and connexin 46 (Cx46) in neonatal rat lung tissue. Neonatal rats were kept in either 21% (normoxia) or 85% O2(hyperoxia) continuously from postnatal day (PN) 1 to 14. The neonatal rats of normoxia group had well-formed alveoli and a normal RAC value. Distal lung histology in neonatal rats in the hyperoxia group showed fewer and larger alveoli with a lower RAC value ($P < 0.01$). Compared with the normoxia group, the ROS level and MDA level were significantly higher ($P < 0.01$), and the GSH level was remarkably lower ($P < 0.01$) in the hyperoxia group. The statistical analysis of TUNEL staining and apoptosis index (AI) results indicated that AI was significantly higher in the hyperoxia group than in the normoxia group ($P < 0.01$). Cx26, Cx32, Cx43, and Cx46 mRNAs levels in the hyperoxia group were higher than those in the normoxia group ($P < 0.01$). Immunohistochemical results suggested that Cx26, Cx32, Cx43, and Cx46 were expressed in the lung tissue of both normoxic and hyperoxic neonatal rats. Immunofluorescence double-staining results suggested that Cx26 was expressed in both alveolar type I (ATI) and alveolar type II (ATII) cells. Nevertheless, its expression was mainly enriched in ATII cells. Cx32 was expressed in ATII cells only. Cx43 was expressed in both ATI and ATII cells. Cx46 was expressed in both ATI and ATII cells, but mainly in ATI cells. The Cx32 mRNA level was positively correlated with ROS level ($P < 0.01$), positively correlated with AI level ($P < 0.01$), and negatively correlated with RAC value ($P < 0.01$). We found that Cx32 was expressed only in ATII cells and was closely related to oxidative stress, apoptosis, and alveolar development. Cx32 may be involved in the development of BPD and may be a novel target for BPD management.

Introduction

Bronchopulmonary dysplasia (BPD) is a chronic lung disease that severely threatens preterm infants' lifespan and affects their quality of life. In recent years, the incidence of BPD has remained high, and various prevention and treatment strategies have failed to mitigate its prevalence effectively [1]. Epidemiological data reveals that the prevalence of BPD in preterm infants born at gestational age of less than 28 weeks ranges from 17–75%, and the younger the gestational age and the lower the birth weight, the higher the incidence [2]. The pathogenesis of BPD is presently recognized as the result of multiple external factors (oxygen toxicity, mechanical ventilation, prenatal or postnatal infections, among others) that damage the developing lungs of preterm infants, inhibit the normal lung development process, and lead to alveolar dysplasia, which is frequently accompanied by pulmonary microangiopathy [3]. As a typical pathological feature, alveolar dysplasia severely impairs pulmonary function in infants with BPD. Its undesirable consequences can persist into adolescence and even adulthood, putting significant health and economic burdens on patients' families and the society. Therefore, investigating the molecular mechanism of alveolar dysplasia in BPD has become a major focus of research in neonatology.

Oxidative stress (OS) is part of the critical pathogenesis of BPD [4–7]. Oxygen inhalation, mechanical ventilation, and infection can cause a surge in the level of reactive oxygen species (ROS) in preterm infants' lungs, which, together with the underdeveloped antioxidant system in preterm infants, further imbalances oxidation and antioxidation, causing oxidative stress damage and worse, death of lung tissue cells [8–9]. It has already been demonstrated that both mechanical ventilation and hyperoxia exposure can increase apoptosis in the lungs of preterm infants [10–11]. As the "stem cells" of alveolar development, alveolar type II (ATII) cells are the primary target cells underlying alveolar dysplasia in BPD [12]. ATII can self-renew or transdifferentiate into ATI cells, with functions including synthesizing and secreting pulmonary surfactant, participating in pulmonary sodium and water transport, and immune regulation [13]. Our research group previously found that increased apoptosis of ATII cells was involved in arresting alveolar development in BPD, and reducing ATII cell apoptosis could significantly improve the outcome of alveolar development in BPD [14]. Therefore, in-depth research on the molecular regulatory mechanism of oxidative stress damage and apoptosis in ATII cells may provide us with a new target and theoretical basis for BPD prevention and treatment.

Intercellular communication plays a vital role shaping human body response to stress and the cells' fate. In response to acute or mild stress, the body will rapidly mobilize the entire intercellular communication network to "dilute" the toxicity within the damaged cells and facilitate their survival (the "Good Samaritan Effect"). However, amid stress that is severe or persistent, the intercellular communication network becomes a medium for spreading and amplifying cytotoxicity, damaging and even killing more cells (the "Bystander Effect") [15–17]. Gap junction channels (GJCs) are transmembrane channels among the most common forms of mediating intercellular communication [18–19]. According to previous studies, GJCs allow pro-apoptotic signaling between cells to trigger increased apoptosis, while GJCs blockers can inhibit intercellular pro-apoptotic signaling, which is beneficial for maintaining cellular homeostasis and reducing apoptosis [20–21]. GJCs are assembled by gap junction proteins (connexins, Cxs). 6 Cxs oligomerize on the cytoplasmic membrane to compose one gap junction hemichannel (HC), and HCs on adjacent cytoplasmic membranes pair up to construct GJCs. Almost all mammalian species express Cxs. Human Cxs have 21 isoforms, with different organs and cells expressing specific Cxs [22]. Cxs expressed by alveolar epithelial cells include: connexin 26 (Cx26), connexin 30 (Cx30), connexin 32 (Cx32), connexin 37 (Cx37), connexin 40 (Cx40), connexin 43 (Cx43), and connexin 46 (Cx46) [23–26]. Since Cx30, Cx37 and Cx40 are expressed at very low levels, alveolar epithelial cells predominantly express Cx26, Cx32, Cx43, and Cx46, Cx32 and Cx43 being the most expressed [23–26]. Physiologically, ATI cells express Cx26, Cx43, and Cx46, with Cx43 expressed predominantly; ATII cells express Cx26, Cx32, Cx43, and Cx46, with Cx26 and Cx32 expressed predominantly and Cx32 expressed only in ATII [23–26]. In contrast, the expression profile of gap junction proteins in alveolar epithelial cells may be altered in pathological conditions. In the bleomycin-induced lung injury model, the expression of Cx43 and Cx46 in alveolar epithelial cells can be significantly increased [24]. It has been reported that Cxs are involved in the onset and progression of several lung diseases, such as pneumonia, asthma, and lung tumors [27–29]. Recognizing the critical actions of Cxs in lung diseases, in this study, we have established an animal model of BPD alveolar

dysplasia simulated by exposing neonatal rats to hyperoxia, and detected the expression of Cx26, Cx32, Cx43, and Cx46 in lung tissues of these neonatal rats, especially in ATII cells, to screen for key Cxs that are likely to be involved in regulating BPD alveolar dysplasia. Meanwhile, we have detected the lung development, oxidative stress level, and apoptosis in lung tissues of these neonatal rats.

Experimental Materials And Methodology

Animal Model and Specimen Collection

As per the BPD animal model previously established by our group [14], SD rats not older than 12 hours after birth were randomly divided into the normoxia group (N group) and hyperoxia group (H group). Neonatal SD rats in the N group (n=30) were placed in a normoxic (21 %, O_2) environment, and neonatal SD rats in the H group (n=30) were housed in a hyperoxic (85 %, O_2) glass chamber. The environmental oxygen concentration was detected by an oxygen concentration detector; the carbon dioxide concentration in the hyperoxic chamber was measured by a gas analyzer, and the carbon dioxide level was maintained at no more than 0.5% by pure alkali-lime; color-changing silica gel was additionally placed in the hyperoxic glass chamber to reduce the environmental humidity. The humidity of the environment was maintained at 60-70 % for both groups, and the ambient temperature was kept at 24-26 °C as well as a 12-hour light-dark cycle. Each mother rat fed 6-8 pups to minimize the effect of nutritional differences on lung development. The mother rats in the N group and H group were replaced per light-dark cycle to avoid poisoning due to over-oxygenation. The bedding was renewed daily with food and water available ad libitum, and each replacement was restricted to half an hour.

In groups N and H, lung tissue specimens were collected from 6 randomly selected pups on postnatal day 1 (PN1d), postnatal day 3 (PN3d), postnatal day 7 (PN7d), and postnatal day 14 (PN14d), respectively. Phenobarbital (1 %, 50 mg/kg) was injected into the abdominal cavity of the pups for anesthesia, the thoracic cavity was cut open, and saline (0.9%) was injected into the heart to flush the heart and lung tissue and remove as much blood as possible. The lung lobes were stripped, and the hilar connective tissue was excised. The lower lobe of the right lung was soaked in paraformaldehyde solution (4 %) for at least 48 hours. The rest lung tissues were transferred to a -80 °C refrigerator for cryopreservation using a liquid nitrogen tank.

HE staining and radial alveolar count (RAC) values

Lung tissue paraffin sections were subjected to HE staining before observed under light microscopy to depict its structure. The RAC value is a quantitative index for evaluating alveolar development. The number of alveoli within a straight-line distance from the center of a respiratory bronchiole to the edge of the lung or to the nearest connective tissue in HE-stained lung tissue sections observed under light microscopy was counted and is defined as the RAC value.

Measurement of ROS levels in lung tissue

Lung tissue homogenates were centrifuged at 4°C, 1000 *g* for 10 minutes, and the supernatants were collected for subsequent assays. A portion of the supernatant was taken to detect the protein concentration, after which the lung tissue supernatant was thoroughly mixed with DCFH-DA working solution, incubated at 37 ℃ for 30 minutes, before the fluorescence intensity of the mixture was measured.

Measurement of MDA levels in the lung tissue

The supernatant of centrifuged lung tissues was added to the working solution from an MDA kit, vortexed and mixed, and boiled in a water bath at 95℃ for 40 minutes. The sample was then removed and cooled under running water, before centrifuged at 4000 *g* for 10 minutes. Finally, the supernatant was removed for absorbance measurement by a microplate reader.

Measurement of GSH levels in lung tissue

The supernatant of centrifuged lung tissues was mixed with the working solution from a GSH kit, centrifuged at 825 *g* for 10 minutes, and left at rest for 10 minutes, before its absorbance was measured with a microplate reader.

TUNEL staining

A lung tissue paraffin section was dewaxed, hydrated, and subjected to antigen repair using an EDTA antigen repair solution. Hydrogen peroxide solution was added dropwise to fully cover the lung tissue, which was then incubated in a wet box for 20 minutes. After shaking off the hydrogen peroxide solution, the lung tissue was rinsed in PBS three times for 5 minutes each. TUNEL reaction solution was drip-fed to the sectioned lung tissue until it was fully covered. The section was incubated in a wet box for 60 minutes. The TUNEL reaction solution was then removed, and the section was rinsed in PBS three times for 5 minutes each. The DAPI solution was added dropwise, and the section was incubated at room temperature for 5 minutes. The section was rinsed in PBS solution for 5 minutes after shaking off the DAPI solution, a procedure that was repeated 3 times. Note that all above operations must be performed without exposure to light. The liquid on the section was removed, and an antifade mounting medium was dripped onto the lung tissue, after which the section was sealed with a coverslip with due care to prevent air bubbles. The apoptosis index (AI) is calculated as the number of positive cells/total cells × 100 %.

Real-time PCR for gene expression assay

After extracting total RNA from lung tissue by adding Trizol and reverse transcribing it to cDNA using a TAKARA reverse transcription kit, quantitative PCR amplification was performed in a 20ul system using a PCR amplification kit with synthetic primers (Cx26: forward: 5'-AGCGTCTGGTGAAGTGTAAC-3', reverse:5'-TTCCCTGAGCAATACCTAAT-3'; Cx32 forward: 5'- TGGTGCGGCTGGTCAAGT-3', reverse: 5'- GGAGGCGG CGAGCATAAA-3'; Cx43: forward: 5'-TCTCGCCTATGTCTCCTCC-3', reverse: 5'-TGGTCCACGATGGCTAAT-3'; Cx46 forward: 5'-TGTGGCTGACCGTCCTGT-3', reverse:5'- AGAAGCGAATGTGCGAGAT-3' β-actin: forward: 5'-CGTGCGTGACATTAAAGAG-3', reverse: 5'-TTGCCGATAGTGATGACCT-3').

Immunohistochemical staining

A lung tissue paraffin section was dewaxed, hydrated, and subjected to antigen repair using an EDTA antigen repair solution. Hydrogen peroxide solution was added dropwise until the lung tissue was adequately covered, and the lung tissue was incubated in a wet box for 20 minutes. After shaking off the hydrogen peroxide solution, the section was rinsed in PBS three times for 5 minutes each. Next, serum was applied dropwise to the sectioned lung tissue until it was well covered. The lung tissue was then incubated in a wet box for 20 minutes before the serum was removed with caution so that it was not rinsed at this point. A primary antibody dilution buffer (Cx26 antibody, 51-2800, Invitrogen, USA; Cx32 antibody, bs-1376R, Bioss, China; Cx43 antibody, bs-0651R, Bioss, China; Cx46 antibody, bs-13363R, Bioss, China) was applied dropwise to the sectioned lung tissue until it was well covered, after which it was incubated in a wet box at 4°C overnight. The next day, after removing the primary antibody dilution buffer, the lung tissue was rinsed 3 times in PBS for 5 minutes each time. The sectioned lung tissue was then treated with a second antibody dilution buffer dropwise until it was fully covered and incubated in a wet box for 20 minutes. After incubation, the secondary antibody dilution buffer was removed, and the lung tissue was rinsed 3 times in PBS for 5 minutes each time. The lung tissue section was then subjected to DAB color development under a light microscope and hematoxylin re-staining before sealed in neutral resin. After that, the stained section was observed under a light microscope.

Immunofluorescence double staining

A lung tissue paraffin section was dewaxed, hydrated, and subjected to antigen repair using an EDTA antigen repair solution. The sectioned lung tissue was covered dropwise with serum until it was fully covered and incubated in a wet box for 20 minutes before removing the serum with caution so that it was not rinsed at this point. The sectioned lung tissue was then covered dropwise with a primary antibody dilution buffer (Cx26 antibody, 51-2800, Invitrogen, USA; Cx32 antibody, bs-1376R, Bioss, China; Cx43 antibody, bs-0651R, Bioss, China; Cx46 antibody, bs-13363R, Bioss, China. p180 antibody, ab24751, Abcam, USA; AQP5 antibody, sc-514022, Santa, USA) until it was well covered, placed in a wet box, and incubated overnight at 4°C. The next day, after removing the primary antibody dilution buffer, the lung tissue was rinsed 3 times in PBS for 5 minutes each time. The sectioned lung tissue was then treated with a second antibody dilution buffer dropwise until it was fully covered and incubated in a wet box for 20 minutes. After incubation, the secondary antibody dilution buffer was removed, and the lung tissue was rinsed 3 times in PBS for 5 minutes each time. After draining the section, a DAPI solvent was applied dropwise to the lung tissue so that it was covered in full and the nuclei could be stained. After dumping off the DAPI solution, the section was rinsed 3 times in PBS for 5 minutes each time. Note that all the above operations must be done without exposure to light. The liquid on the section was then removed, and an antifade mounting medium was dripped onto the lung tissue, after which the section was sealed with a coverslip with due care to avoid air bubbles. Finally, the stained section was observed for fluorescence using a confocal microscope.

Statistical analysis

Graph Pad Prism 8 software was applied for statistical analysis and graph preparation; all data were presented as mean ± standard deviation. Comparisons between the two groups were performed by t-test, and correlation analysis was conducted using the Pearson correlation coefficient methodology. Differences were considered statistically significant when $P < 0.05$.

Results

Hyperoxia exposure induces alveolar hypoplasia in neonatal rats

The HE staining results (Figure 1A) showed that alveolarization in group N was well developed, as evidenced by a gradual increase in the number of alveoli, a gradual decrease in the volume of alveoli, a gradual uniform and regular alveolar morphology. In contrast, group H exhibited alveolar dysplasia, characterized by the reduced alveolar number, increased alveolar volume, and simplified alveolar structure, in accordance with the pathological alterations in BPD alveolar dysplasia. The neonatal rats exposed with had a higher RAC value than those with hyperoxia exposure (Figure 1 B, $P < 0.01$).

Hyperoxia exposure increases the level of oxidative and apoptosis in neonatal rat lung tissue

In comparison with group N, after 14 days of hyperoxia exposure, ROS levels (Figure 2 A, $P < 0.01$) and MDA levels in the lung tissue were significantly higher (Figure 2 B, $P < 0.01$), while GSH levels in the lung tissue were remarkably lower in group H neonatal rats (Figure 2 C, $P < 0.01$). Moreover, the number of TUNEL-positive cells in the lung tissue was significantly higher in group H after 14 days of hyperoxia exposure compared with group N (Figure 3 A). In addition, the apoptosis index (AI) was much higher in group H than in group N (Figure 3 B, $P < 0.01$).

Hyperoxia exposure upregulates Cx26, Cx32, Cx43, and Cx46 expression in neonatal rat lung tissue

We quantified Cx26, Cx32, Cx43, and Cx46 mRNA expression levels with real-time PCR. With the exception of the Cx26 mRNA level in group H on day 3 after birth, which was lower than that in group N (Figure 4A, $P < 0.01$), Cx26 mRNA levels in group H on day 1, day 7, and day 14 after birth were all higher than those in group N (Figure 4 A, $P < 0.01$); Cx32 mRNA levels in group H on day 1, day 3, day 7 and day 14 after birth were all higher than those in group N (Figure 4 B, $P < 0.01$); Cx43 mRNA levels in group H on day 1, day 3, day 7 and day 14 after birth were all higher than those in group N (Figure 4 C, $P < 0.01$); and Cx46 mRNA levels in group H on day 1, day 3, day 7 and day 14 after birth were all higher than those in group N (Figure 4D, $P < 0.01$). We further measured the expression of Cx26, Cx32, Cx43, and Cx46 in neonatal rat lung tissue by immunohistochemical staining and immunofluorescence double-staining. The immunohistochemical staining results suggested (Figure 5-8) that Cx26, Cx32, Cx43 and Cx46 were all expressed in neonatal rat lung tissue, and the results by 1000x oil microscopy indicated that Cx26, Cx32, Cx43, and Cx46 were widely expressed in the cell membrane, cytoplasm, and nucleus. In addition, we observed the expression of Cx26, Cx32, Cx43, and Cx46 in ATI and ATII cells using immunofluorescence double-staining. The results showed that Cx26 was expressed in both ATI and ATII, but mainly in ATII cells

(Figure 9); Cx32 was expressed in ATII cells only (Figure 10); Cx43 was expressed in both ATI and ATII cells (Figure 11); Cx46 was expressed in both ATIand ATII, but mainly in ATI cells (Figure 12).

Correlation analysis between Cx32 mRNA level and ROS level, apoptosis index (AI), and RAC value

Using the Pearson correlation coefficient method, we have analyzed the correlation between Cx32 mRNA level and ROS level, AI, and RAC value, and revealed a positive correlation between Cx32 mRNA level and ROS level (Figure 13 A, $P < 0.0001$), a positive correlation between Cx32 mRNA level and AI (Figure 13 B, $P < 0.0001$), and a negative correlation between Cx32 mRNA level and RAC value (Figure 13 C, $P < 0.0001$).

Discussion

In this study, the rat model of BPD was developed by exposing neonatal rats to a hyperoxic environment. Hyperoxia exposure increased oxidative stress and apoptosis levels in the lung tissue of neonatal rats and arrested the alveolar development of neonatal rats. We further investigated the expression of Cx26, Cx32, Cx43 and Cx46 in neonatal rat lung tissue. The results of real-time PCR showed that the expression levels of Cx26, Cx32, Cx43, and Cx46 genes in the hyperoxia group were significantly higher than those in the normoxia group. Immunohistochemical results showed that Cx26, Cx32, Cx43, and Cx46 were expressed in lung tissues of neonatal rats with normoxic and hyperoxic exposure. Immunofluorescence double-staining results confirmed that ATI cells expressed Cx26, Cx43 and Cx46, while ATII cells expressed Cx26, Cx32, Cx43 and Cx46, with Cx32 being expressed only in ATII cells. In addition, the Cx32 mRNA level was closely correlated with ROS level, AI index, and RAC value. Therefore, we believe that hyperoxia exposure increases the expression of Cx26, Cx32, Cx43 and Cx46, and that Cx32 may be closely related to oxidative stress, apoptosis and alveolar development, suggesting that Cx32 is likely involved in the development of BPD and could be a novel target for BPD management.

Each year, 15 million infants are born prematurely worldwide, which is approximately one-tenth of all births [30]. In the last 50 years, there has been tremendous progress in the management strategies for preterm infants, and the survival rate of extremely and very low birth weight infants has been on the rise, albeit the incidence of BPD remains high. Infants with BPD suffer from not only the significantly poor pulmonary function but also other systemic conditions, such as cardiac insufficiency, retinopathy, and delayed neurological development [31–32]. Therefore, BPD has become a major contributor to the poor prognosis of extremely and very low birth weight infants, putting heavy health and economic burdens on the patients' families and the society. Therefore, a more in-depth understanding of the molecular regulatory mechanisms underlying the development of BPD can help identify new targets and provide a new theoretical basis for BPD prevention and treatment.

The development of fetal lungs can be divided into five different periods, namely the embryonic, pseudoglandular, canalicular, saccular, and alveolar periods [33]. Most preterm infants with BPD are born in the saccular period and develop typical histopathological changes of BPD lungs during the alveolar period [34]. The primary reason for the occurrence of alveolar dysplasia in BPD infants is that the lungs of

preterm infants are still in the saccular phase, with immature anatomical structures and physiological functions, making them highly susceptible to infection, hyperoxia, mechanical ventilation, and other influences, resulting in abnormal sequences and orientations of lung development and difficulties in completing normal growth and development through the alveolar period. Therefore, identifying the key molecular mechanisms underlying alveolar dysplasia has long been a topical research topic in the pathogenesis of BPD. An animal model of BPD is essential to developed a better understanding of the pathogenesis of BPD. Oxygen toxicity is an important trigger for BPD in preterm infants. Even when preterm infants are given the minimum required oxygen supplementation while a lung ventilation protection strategy is implemented, it is still strong enough to induce oxidative stress and cause lung injury [35–36]. The rodent BPD model established by hyperoxia exposure can well mimic the pathological changes of BPD in human preterm infants, which can help shape a better understanding of the pathogenesis of BPD and examine the therapeutic efficacy of anti-BPP approaches [37–40]. In this study, we placed neonatal rats within 12 hours after their birth in a hyperoxic environment (85% O_2) until day 14 after birth. HE staining confirmed that the histopathological changes in their lungs were consistent with alveolar dysplasia in BPD, as demonstrated by a radical decrease in the number of alveoli, a dramatic increase in alveolar volume, the absence of secondary alveolar septa, the simplification of alveolar structure, and a significant decrease in the RAC value.

Clinical studies have confirmed that the levels of oxidative stress markers 8-OHDG and MDA in plasma or bronchoalveolar lavage fluid of preterm infants ultimately diagnosed with BPD were significantly higher than those of non-BPD preterm infants within 1 week after birth, in contrast to a significantly lower level of the antioxidant GSH than that in non-BPD preterm infants [41–43]. The results of this study also demonstrate that the levels of ROS and MDA in lung tissues of hyperoxia-exposed rats were significantly higher, while the GSH level was much lower, indicating that oxidative stress was induced in lung tissues of BPD rats. Therefore, antioxidant therapies may be effective in preventing and treating BPD. However, studies on antioxidant therapy against BPD have not provided a definite answer. The administration of ROS scavengers or antioxidant enzyme supplements in preterm infants in the early postnatal period has failed to reduce the incidence of BPD significantly, although it alleviated the clinical symptoms of BPD in preterm infants to a certain extent [44–47]. In this regard, people seek to improve the current antioxidant treatment regimen for preterm infants and identify new therapeutic strategies for preventing and treating BPD by gaining insight into the molecular regulatory network underlying the development of oxidative stress-induced BPD. Oxidative stress-induced apoptosis has been proven for its involvement in the onset and progress of several diseases. Apoptosis is essential in normal cell turnover, tissue development, and injury repair. A significant decrease or an excessive increase in apoptosis can lead to developmental disorders or abnormal damage repair in organs or tissues. In this study, we have assessed the apoptosis in the lung tissue through TUNEL staining and AI, and confirmed that the AI in lung tissues of group H was significantly higher than that of group N. To sum up, this study confirms that oxidative stress is triggered while apoptosis is significantly increased in lung tissues of hyperoxia-exposed neonatal rats.

Gap junction channels (GJCs) are one of the most common forms that constitute intercellular communication networks. GJCs are composed of gap junction proteins (connexins, Cxs) that can directly connect the cytoplasm of adjacent cells, allowing direct cell-to-cell transmission and exchange of various ions, nutrients, and second messengers, such as Ca^{2+}, ATP, cAMP, IP_3, amino acids, NO, and GSH. Cxs and GJCs serve as essential regulators in the respiratory system. They are indispensable in physiological conditions while playing an important role in pathological conditions such as the response of the organism to environmental stress [23]. The GJCs facilitate intercellular calcium wave transmission in bronchioles, which contributes to synchronized ciliary motility, thus allowing for targeted transport of mucus for the removal of toxins and microorganisms from the environment. In alveolar epithelial cells, intracellular calcium concentration is increased by mechanical stimulation affecting ATI cells, which in turn triggers the secretion of lung surface active substances by ATII cells by transmitting calcium waves to ATII cells via GJCs. In pulmonary capillaries, pulmonary endothelial cells can transmit pro-inflammatory signals via GJCs and upregulate the expression of P-selectin on the cytoplasmic membrane, which induces an inflammatory response.

Alveoli are the gas exchange units of the lung tissue. Disturbances in alveolar development can directly lead to abnormal gas exchange, which is one of the main pathological changes in BPD. Alveolar epithelial cells are the key target cells in BPD alveolar dysplasia. Alveolar epithelial cells comprise ATI and ATII cells. ATI cells are large and extremely flat, occupying more than 90% of the alveolar area and playing an essential role in the gas exchange process. However, AT II cells, the "progenitor" cells of alveolar development, are approximately twice as many as ATI cells. By means of freeze-fracture electron microscopy, the interconnectivity of alveolar epithelial cells through gap junction channels has long been demonstrated [48]. Each AT I cell shares gap junction channels with at least one AT I cell and one AT II cell. Among the 21 Cxs expressed in mammals, alveolar epithelial cells mainly express Cx26, Cx32, Cx43, and Cx46. Among them, AT I cells express Cx26, Cx43 and Cx46, with Cx43 being expressed predominantly. ATII cells, on the other hand, express Cx26, Cx32, Cx43 and Cx46, with Cx26 and Cx32 expressed predominantly and Cx32 expressed only in AT II cells. Cx43 is the most widely expressed Cx in mammals and is expressed in both AT I and AT II cells. However, in adult rat lung tissues, Cx32 is expressed only in ATII cells, and it may be involved in constituting inter-ATII GJCs. Interestingly, ATI cells cannot form GJCs with cells expressing only Cx32 [24]. Thus, ATII cells have two independent types of GJCs, Cx43-compatible GJCs and Cx32-compatible GJCs, whereas AT I cells have only Cx43-compatible GJCs. This suggests that in normal lung tissues, ATI-ATII intercellular communication mainly depends on Cx43-compatible GJCs; by contrast, ATII-ATII cells have independent intercellular channels, i.e., Cx32-compatible GJCs, which are not available for communication between ATII cells and ATI cells. However, in normal lung tissues, ATII cells can hardly connect directly with ATII cells to form inter-ATII GJCs. Therefore, Cx32 appears to play a smaller role than Cx43 in undamaged lung tissues. However, it has been reported that in damaged lung tissues, there is an increased chance of direct ATII-ATII connections, and Cx32-compatible GJCs may form a "priority" inter-ATII channel [23–24]. Thus, Cx32 plays a special part in the connection between ATIIcells and the outside world and may have unexpected effects, especially when alveolar epithelial cells are damaged.

To quantify the expression of Cx26, Cx32, Cx43 and Cx46 in lung tissues, we have performed real-time PCRs on neonatal rat lung tissues, and results revealed that Cx26, Cx32, Cx43 and Cx46 mRNA levels were significantly higher in neonatal rat lung tissue in the hyperoxia group than in the normoxia group. In this study, we have confirmed based on immunohistochemical results that Cx26, Cx32, Cx43 and Cx46 were expressed in both normoxia and hyperoxia exposed neonatal rat lung tissue. We used immunofluorescence double-staining to identify ATI and ATII on lung tissue sections and simultaneously detect the expression of Cx26, Cx32, Cx43, and Cx46. The immunofluorescence double-staining results confirmed that Cx26 was expressed in both ATI and ATII cells, with expression mainly in ATII cells; Cx32 was expressed only in ATII cells; Cx43 was expressed in both ATI and ATII cells; and Cx46 was expressed in both ATI and ATII cells, with expression mainly in ATI cells. These results align with those reported in past literature [23–24] that ATIcells predominantly express Cx43, while Cx32 is expressed only in ATII cells. We then analyzed Cx32 mRNA level with ROS level, AI level, and RAC value by the Pearson correlation coefficient methodology, and revealed a positive correlation between Cx32 mRNA level and ROS level, a positive correlation between Cx32 mRNA level and AI, and a negative correlation between Cx32 mRNA level and RAC value. The above results indicate that in hyperoxia-exposed neonatal rat lung tissue, Cx32 may be associated with oxidative stress and apoptosis and may be involved in the development of alveolar dysplasia in BPD.

This study has several limitations. First, BPD is a multi-factorial disease, and oxygen toxicity is only one of the many contributing factors; infection and ventilator-related volume/pressure injury can all fuel the development of BPD. In this study, we have only established a hyperoxia-exposed neonatal rat model to simulate BPD. Therefore, other BPD models are needed to further clarify the expression and effects of gap junction proteins in BPD. Second, this study lacks in vitro experiments on ATII cells, and the expression of Cxs in ATII cells has not been confirmed in vitro. In addition, the effects of Cx32 in BPD deserve further investigation, and the role that Cx32 plays in BPD has not been well defined in this study. Targeted intervention on Cx32 at the animal or cellular level may help to specify the effects of Cx32 in BPD and the mechanism underlying its actions.

Conclusion

In neonatal rats exposed to hyperoxia, the alveoli are poorly developed, and the levels of oxidative stress and apoptosis in the lung tissue significantly increase. Cx26, Cx32, Cx43 and Cx46 are all highly expressed in the lung tissue of neonatal rats exposed to hyperoxia, while Cx32 is only expressed in ATII cells and is closely associated with oxidative stress, apoptosis, and alveolar development. Cx32 is likely to be involved in the development of BPD and could be a new target for BPD management.

Declarations

FUNDING

This study was supported by grants from Liaoning Providence Science and Technology project (2020JN1/10300001).

AVAILABILITY OF DATA AND MATERIALS

The datasets used and/or analyzed during the current study are available from the corresponding author on reasonable request.

DECLARATIONS

AUTHOR CONTRIBUTION

QC, XX, and JF conceived and designed the study. QC and XY performed the experiments. QC and XY analyzed the data. XX and JF reviewed the data. QC wrote the manuscript. All authors read and approved the final manuscript.

Ethics Approval and Consent to Participate

All animal procedures were approved by the ethics committee of China Medical University (Approval No.: 2021PS267K) and followed institutional guidelines. All animal procedures also

followed ARRIVE guidelines.

Acknowledgements

Not Applicable

Consent for Publication

Not Applicable.

Competing Interests

The authors declare no competing interests.

References

1. Gilfillan Margaret., Bhandari Anita., Bhandari Vineet.(2021). Diagnosis and management of bronchopulmonary dysplasia. BMJ, 375(undefined), n1974. doi:10.1136/bmj.n1974
2. Siffel, C., Kistler, K. D., Lewis, J. F. M., and Sarda, S. P. (2021). Global Incidence of Bronchopulmonary Dysplasia Among Extremely Preterm Infants: a Systematic Literature Review. J. Maternal-Fetal Neonatal Med. 34 (11), 1721–1731. doi:10.1080/14767058.2019.1646240
3. Thébaud Bernard., Goss Kara N., Laughon Matthew., Whitsett Jeffrey A., Abman Steven H., Steinhorn Robin H., Aschner Judy L., Davis Peter G., McGrath-Morrow Sharon A., Soll Roger F., Jobe Alan H.

(2019). Bronchopulmonary dysplasia. Nat Rev Dis Primers, 5(1), 78. doi:10.1038/s41572-019-0127-7

4. Morty Rory E.(2018). Recent advances in the pathogenesis of BPD. Semin Perinatol, 42(7), 404-412. doi:10.1053/j.semperi.2018.09.001
5. Ozsurekci Yasemin., Aykac Kubra.(2016). Oxidative Stress Related Diseases in Newborns. Oxid Med Cell Longev, 2016(undefined), 2768365. doi:10.1155/2016/2768365
6. Perrone Serafina., Tataranno Maria Luisa., Buonocore Giuseppe.(2012). Oxidative stress and bronchopulmonary dysplasia. J Clin Neonatol, 1(3), 109-14. doi:10.4103/2249-4847.101683
7. Wang Junyi., Dong Wenbin.(2018). Oxidative stress and bronchopulmonary dysplasia. Gene, 678(undefined), 177-183. doi:10.1016/j.gene.2018.08.031
8. Kinsella John P., Greenough Anne., Abman Steven H.(2006). Bronchopulmonary dysplasia. Lancet, 367(9520), 1421-31. doi:10.1016/S0140-6736(06)68615-7
9. Negi Reena., Pande Deepti., Kumar Ashok., Khanna Ranjana S., Khanna H D.(2012). Evaluation of biomarkers of oxidative stress and antioxidant capacity in the cord blood of preterm low birth weight neonates. J Matern Fetal Neonatal Med, 25(8), 1338-41. doi:10.3109/14767058.2011.633672
10. May M., Ströbel P., Preisshofen T., Seidenspinner S., Marx A., Speer C P.(2004). Apoptosis and proliferation in lungs of ventilated and oxygen-treated preterm infants. Eur Respir J, 23(1), 113-21. doi:10.1183/09031936.03.00038403
11. Hargitai B., Szabó V., Hajdú J., Harmath A ., Pataki M., Farid P., Papp Z., Szende B.(2001). Apoptosis in various organs of preterm infants: histopathologic study of lung, kidney, liver, and brain of ventilated infants. Pediatr Res, 50(1), 110-4. doi:10.1203/00006450-200107000-00020
12. Lignelli Ettore., Palumbo Francesco., Myti Despoina., Morty Rory E.(2019). Recent advances in our understanding of the mechanisms of lung alveolarization and bronchopulmonary dysplasia. Am J Physiol Lung Cell Mol Physiol, 317(6), L832-L887. doi:10.1152/ajplung.00369.2019
13. Choi Jinwook., Park Jong-Eun., Tsagkogeorga Georgia., Yanagita Motoko., Koo Bon-Kyoung., Han Namshik., Lee Joo-Hyeon.(2020). Inflammatory Signals Induce AT2 Cell-Derived Damage-Associated Transient Progenitors that Mediate Alveolar Regeneration. Cell Stem Cell, 27(3), 366-382.e7. doi:10.1016/j.stem.2020.06.020
14. Zhang Dan., Wu Linlin., Du Yanna., Zhu Yuting., Pan Bingting., Xue Xindong., Fu Jianhua.(2018). Autophagy inducers restore impaired autophagy, reduce apoptosis, and attenuate blunted alveolarization in hyperoxia-exposed newborn rats. Pediatr Pulmonol, 53(8), 1053-1066. doi:10.1002/ppul.24047
15. Perez Velazquez Jose L., Frantseva Marina V., Naus Christian C.(2003). Gap junctions and neuronal injury: protectants or executioners? Neuroscientist, 9(1), 5-9. doi:10.1177/1073858402239586
16. Spray David C., Hanstein Regina., Lopez-Quintero Sandra V., Stout Randy F., Suadicani Sylvia O., Thi Mia M.(2013). Gap junctions and Bystander Effects: Good Samaritans and executioners. Wiley Interdiscip Rev Membr Transp Signal, 2(1), 1-15. doi:10.1002/wmts.72
17. Zhang Kai., Guan Qi-Wen., Zhou Xin-Yu., Xia Qin-Xuan., Yin Xi-Xi., Zhou Hong-Hao., Mao Xiao-Yuan.(2021). The mutual interplay of redox signaling and connexins. J Mol Med (Berl), 99(7), 933-941.

doi:10.1007/s00109-021-02084-0

18. Goodenough Daniel A., Paul David L.(2009). Gap junctions. Cold Spring Harb Perspect Biol, 1(1), a002576. doi:10.1101/cshperspect.a002576
19. Delvaeye Tinneke., Vandenabeele Peter., Bultynck Geert., Leybaert Luc., Krysko Dmitri V.(2018). Therapeutic Targeting of Connexin Channels: New Views and Challenges. Trends Mol Med, 24(12), 1036-1053. doi:10.1016/j.molmed.2018.10.005
20. Kameritsch P., Khandoga N., Pohl U., Pogoda K.(2013). Gap junctional communication promotes apoptosis in a connexin-type-dependent manner. Cell Death Dis, 4(undefined), e584. doi:10.1038/cddis.2013.105
21. Tirosh Amir., Tuncman Gurol., Calay Ediz S., Rathaus Moran., Ron Idit., Tirosh Amit., Yalcin Abdullah., Lee Yankun G., Livne Rinat., Ron Sophie., Minsky Neri., Arruda Ana Paula., Hotamisligil Gökhan S.(2021). Intercellular Transmission of Hepatic ER Stress in Obesity Disrupts Systemic Metabolism. Cell Metab, 33(2), 319-333.e6. doi:10.1016/j.cmet.2020.11.009
22. Koval Michael., Molina Samuel A., Burt Janis M.(2014). Mix and match: investigating heteromeric and heterotypic gap junction channels in model systems and native tissues. FEBS Lett, 588(8), 1193-204. doi:10.1016/j.febslet.2014.02.025
23. Johnson Latoya N., Koval Michael.(2009). Cross-talk between pulmonary injury, oxidant stress, and gap junctional communication. Antioxid Redox Signal, 11(2), 355-67. doi:10.1089/ars.2008.2183
24. Abraham V., Chou M L., George P., Pooler P., Zaman A., Savani R C., Koval M.(2001). Heterocellular gap junctional communication between alveolar epithelial cells. Am J Physiol Lung Cell Mol Physiol, 280(6), L1085-93. doi:10.1152/ajplung.2001.280.6.L1085.
25. Koval Michael.(2002). Sharing signals: connecting lung epithelial cells with gap junction channels. Am J Physiol Lung Cell Mol Physiol, 283(5), L875-93. doi:10.1152/ajplung.00078.2002
26. osa Davide., Chanson Marc.(2015). The lung communication network. Cell Mol Life Sci, 72(15), 2793-808. doi:10.1007/s00018-015-1960-9
27. Huang Jian-Qiang., Chen Xiao-Yang., Huang Fang., Fan Ji-Min., Shi Xiao-Wei., Ju Yan-Kai.(2018). Effects of Connexin 43 Inhibition in an Ovalbumin-induced Mouse Model of Asthma. Iran J Allergy Asthma Immunol, 17(1), 29-38.
28. Westphalen Kristin., Gusarova Galina A., Islam Mohammad N., Subramanian Manikandan., Cohen Taylor S., Prince Alice S., Bhattacharya Jahar.(2014). Sessile alveolar macrophages communicate with alveolar epithelium to modulate immunity. Nature, 506(7489), 503-6. doi:10.1038/nature12902
29. King Timothy J., Lampe Paul D.(2004). The gap junction protein connexin32 is a mouse lung tumor suppressor. Cancer Res, 64(20), 7191-6. doi:10.1158/0008-5472.CAN-04-0624
30. Blencowe Hannah., Cousens Simon., Oestergaard Mikkel Z., Chou Doris., Moller Ann-Beth., Narwal Rajesh., Adler Alma., Vera Garcia Claudia., Rohde Sarah., Say Lale., Lawn Joy E.(2012). National, regional, and worldwide estimates of preterm birth rates in the year 2010 with time trends since 1990 for selected countries: a systematic analysis and implications. Lancet, 379(9832), 2162-72. doi:10.1016/S0140-6736(12)60820-4

31. araldi Eugenio., Filippone Marco.(2007). Chronic lung disease after premature birth. N Engl J Med, 357(19), 1946-55. doi:10.1056/NEJMra067279
32. Jobe Alan H., Abman Steven H.(2019). Bronchopulmonary Dysplasia: A Continuum of Lung Disease from the Fetus to the Adult. Am J Respir Crit Care Med, 200(6), 659-660. doi:10.1164/rccm.201904-0875ED
33. Joshi Suchita., Kotecha Sailesh.(2007). Lung growth and development. Early Hum Dev, 83(12), 789-94. doi:10.1016/j.earlhumdev.2007.09.007
34. Endesfelder Stefanie., Strauß Evelyn., Bendix Ivo., Schmitz Thomas., Bührer Christoph.(2020). Prevention of Oxygen-Induced Inflammatory Lung Injury by Caffeine in Neonatal Rats. Oxid Med Cell Longev, 2020(undefined), 3840124. doi:10.1155/2020/3840124
35. Ozsurekci Yasemin., Aykac Kubra.(2016). Oxidative Stress Related Diseases in Newborns. Oxid Med Cell Longev, 2016(undefined), 2768365. doi:10.1155/2016/2768365
36. errone Serafina., Bracciali Carlotta., Di Virgilio Nicola., Buonocore Giuseppe.(2016). Oxygen Use in Neonatal Care: A Two-edged Sword. Front Pediatr, 4(undefined), 143. doi:10.3389/fped.2016.00143
37. Nardiello Claudio., Mižíková Ivana., Morty Rory E.(2017). Looking ahead: where to next for animal models of bronchopulmonary dysplasia? Cell Tissue Res, 367(3), 457-468. doi:10.1007/s00441-016-2534-3
38. O'Reilly Megan., Thébaud Bernard.(2014). Animal models of bronchopulmonary dysplasia. The term rat models. Am J Physiol Lung Cell Mol Physiol, 307(12), L948-58. doi:10.1152/ajplung.00160.2014
39. Berger Jessica., Bhandari Vineet.(2014). Animal models of bronchopulmonary dysplasia. The term mouse models. Am J Physiol Lung Cell Mol Physiol, 307(12), L936-47. doi:10.1152/ajplung.00159.2014
40. Buczynski Bradley W., Maduekwe Echezona T., O'Reilly Michael A.(2013). The role of hyperoxia in the pathogenesis of experimental BPD. Semin Perinatol, 37(2), 69-78. doi:10.1053/j.semperi.2013.01.002
41. Millán Iván., Piñero-Ramos José David., Lara Inmaculada., Parra-Llorca Anna., Torres-Cuevas Isabel., Vento Máximo.(2018). Oxidative Stress in the Newborn Period: Useful Biomarkers in the Clinical Setting. Antioxidants (Basel), 7(12), undefined. doi:10.3390/antiox7120193
42. Fabiano Adele., Gavilanes Antonio W D., Zimmermann Luc J I., Kramer Boris W., Paolillo Piermichele., Livolti Giovanni., Picone Simonetta., Bressan Katia., Gazzolo Diego.(2016). The development of lung biochemical monitoring can play a key role in the early prediction of bronchopulmonary dysplasia. Acta Paediatr, 105(5), 535-41. doi:10.1111/apa.13233
43. Ferrante Giuliana., Carota Giuseppe., Li Volti Giovanni., Giuffrè Mario.(2021). Biomarkers of Oxidative Stress for Neonatal Lung Disease. Front Pediatr, 9(undefined), 618867. doi:10.3389/fped.2021.618867
44. Davis Jonathan M., Parad Richard B., Michele Theresa., Allred Elizabeth., Price Anita., Rosenfeld Warren., North American Recombinant Human CuZnSOD Study Group.(2003). Pulmonary outcome

at 1 year corrected age in premature infants treated at birth with recombinant human CuZn superoxide dismutase. Pediatrics, 111(3), 469-76. doi:10.1542/peds.111.3.469

45. Poggi Chiara., Dani Carlo.(2014). Antioxidant strategies and respiratory disease of the preterm newborn: an update. Oxid Med Cell Longev, 2014(undefined), 721043. doi:10.1155/2014/721043
46. D'Angelo Gabriella., Chimenz Roberto., Reiter Russel J., Gitto Eloisa.(2020). Use of Melatonin in Oxidative Stress Related Neonatal Diseases. Antioxidants (Basel), 9(6), undefined. doi:10.3390/antiox9060477
47. Davis J M., Richter S E., Biswas S., Rosenfeld W N., Parton L., Gewolb I H., Parad R., Carlo W., Couser R J., Baumgart S., Atluru V., Salerno L., Kassem N.(2000). Long-term follow-up of premature infants treated with prophylactic, intratracheal recombinant human CuZn superoxide dismutase. J Perinatol, 20(4), 213-6. doi:10.1038/sj.jp.7200363
48. Schneeberger E E., Walters D V., Olver R E.(1978). Development of intercellular junctions in the pulmonary epithelium of the foetal lamb. J Cell Sci, 32(undefined), 307-24. doi:10.1242/jcs.32.1.307

Figures

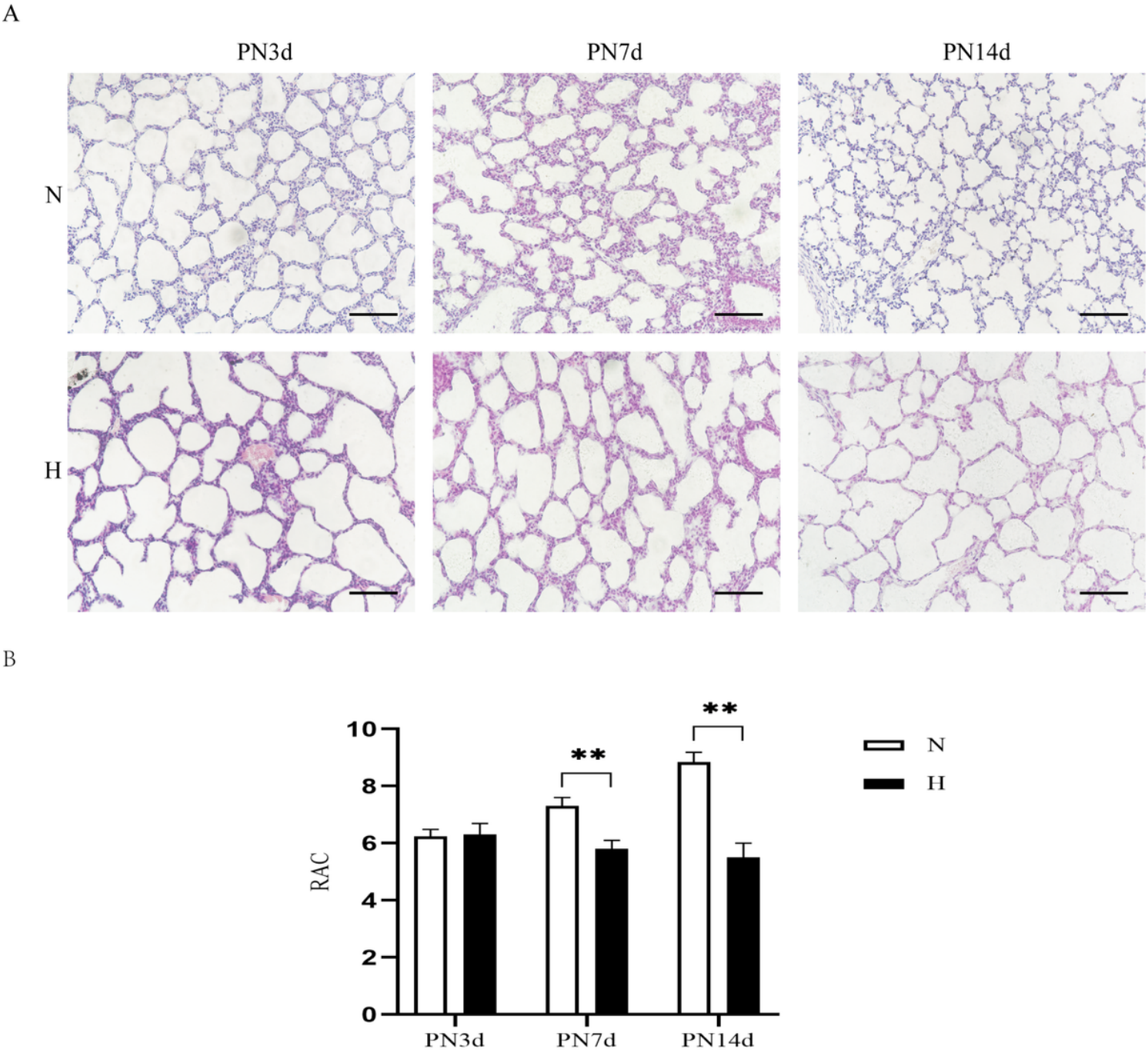

Figure 1

Morphological changes of lung tissue

A: HE staining of lung tissue sections (200 × Scale 100 μ m) . B: RAC value of lung tissue. N: Normoxia group; H: Hyperoxia group; RAC: radial alveolar count; PN1d: 1 day after birth; PN7d: 7 days after birth; PN14d: 14 days after birth;** $P < 0.01$.

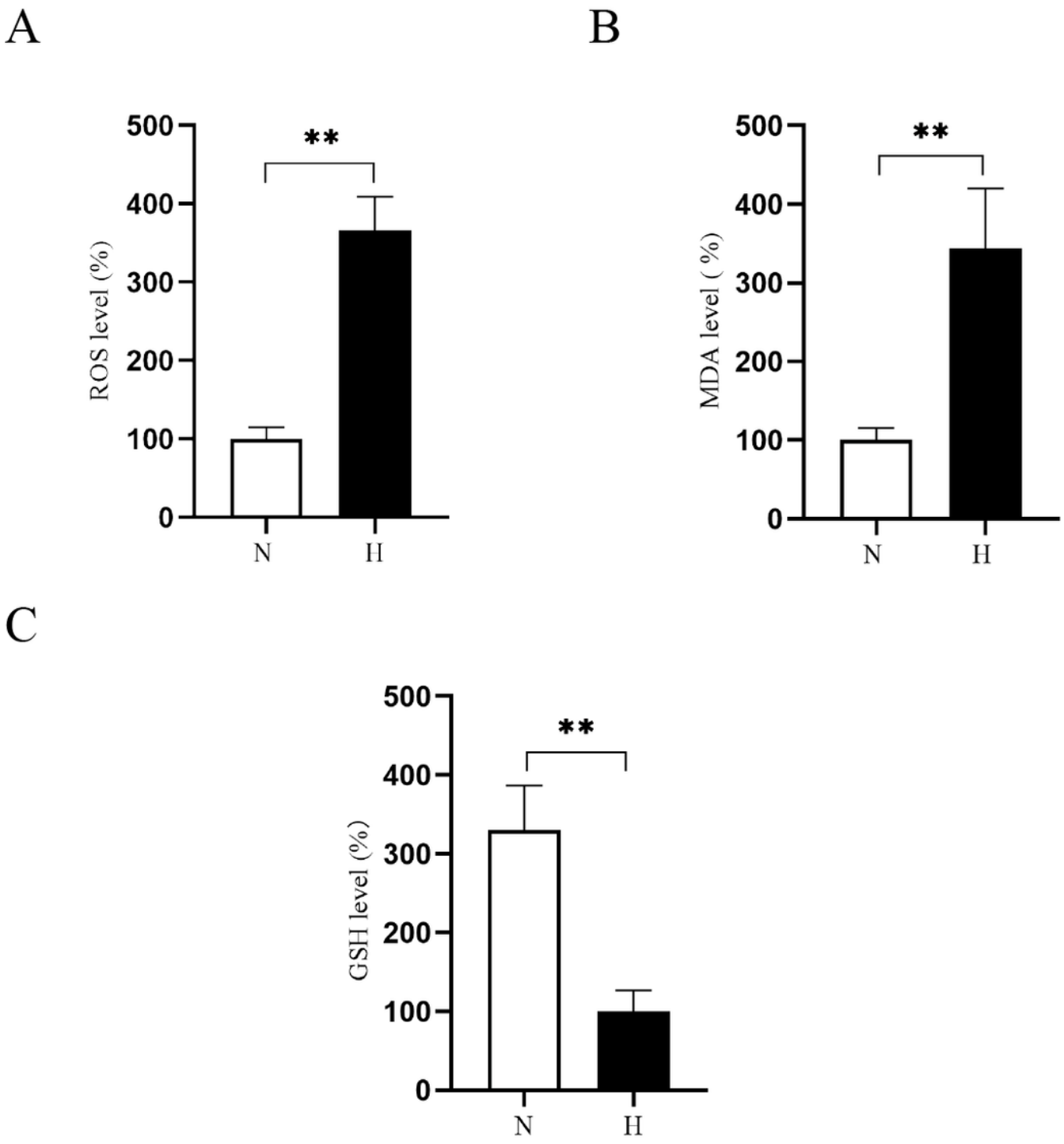

Figure 2

ROS, MDA and GSH levels in lung tissue of neonatal rats on day 14 after birth

A: ROS level (%). B: MDA level(%). C: GSH level (%). N: Normoxia group; H: Hyperoxia group; ROS: reactive oxygen species; MDA: malondialdehyde; GSH: glutathione; ** $P < 0.01$.

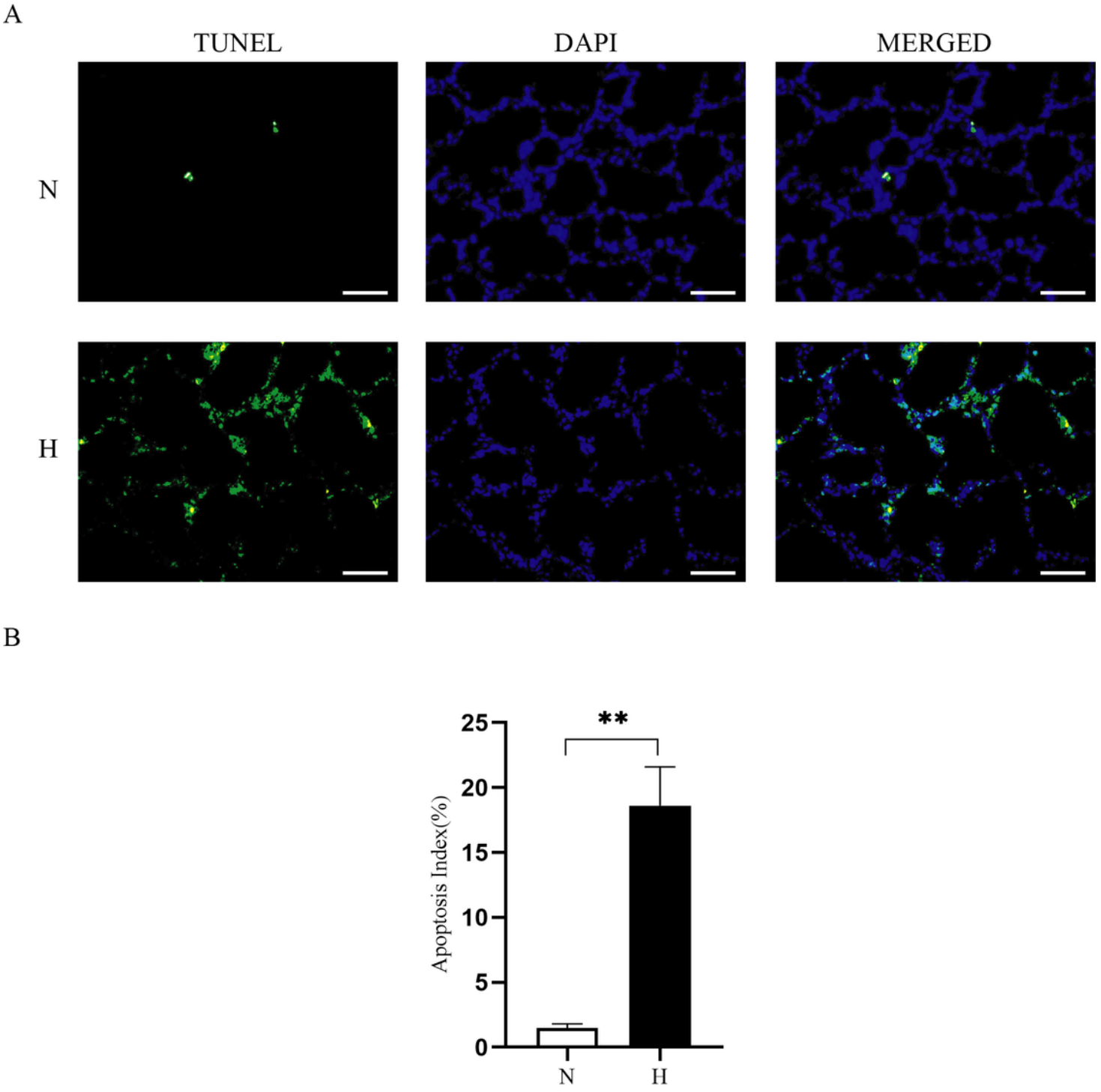

Figure 3

TUNEL staining of lung tissue of neonatal rats 14 days after birth (400 × Scale 50 μ m)

A: TUNEL staining of lung tissue.B: Apoptosis index (AI). Green fluorescence represents TUNEL; Blue fluorescence represents the nucleus; N: Normoxia group; H: Hyperoxia group; AI: apoptosis index;** $P < 0.01$.

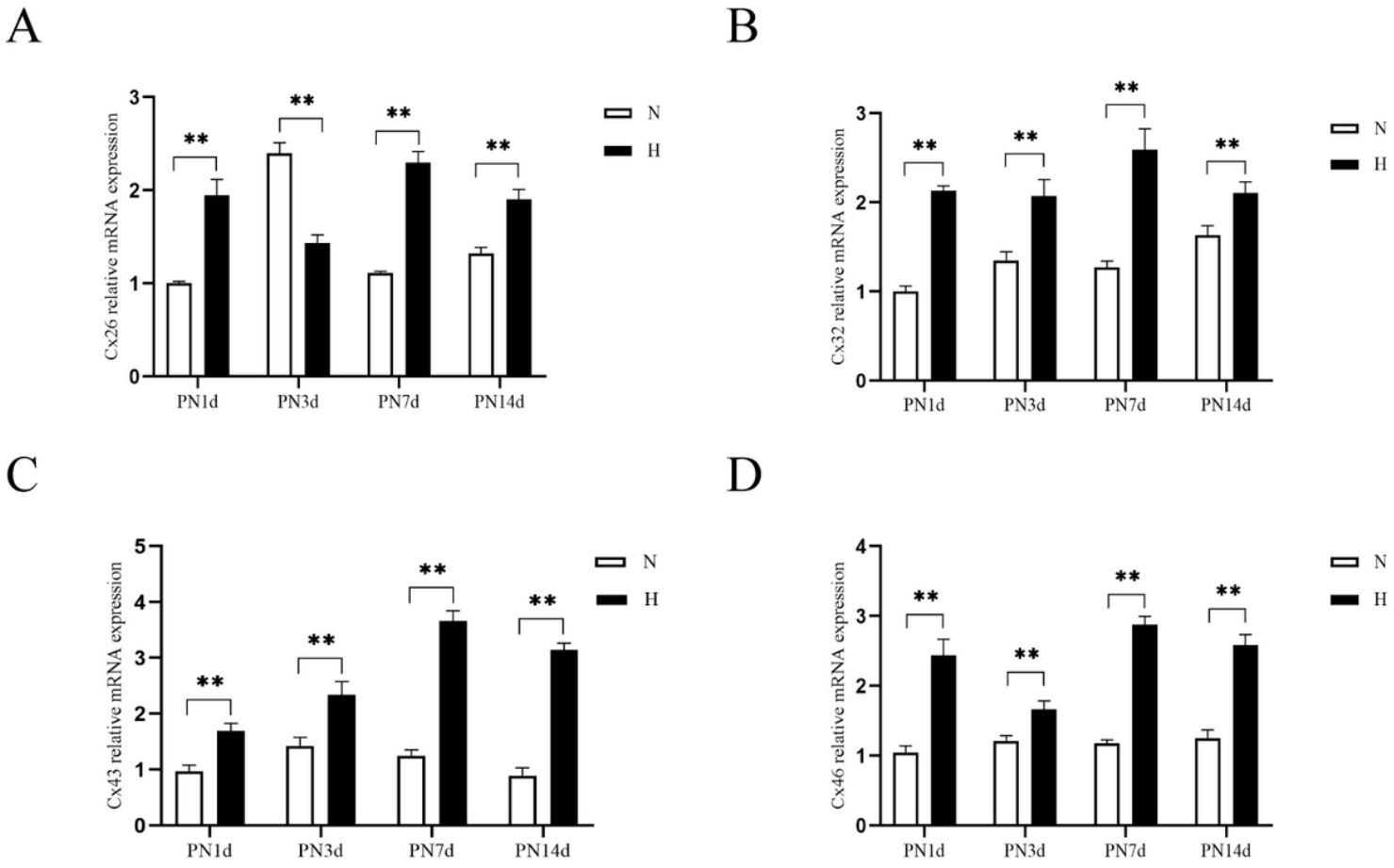

Figure 4

Cx26, Cx32, Cx43 and Cx46 mRNA level in lung tissue of neonatal rats

A: Cx26 mRNA expression. B: Cx32 mRNA expression. C: Cx43 mRNA expression. D: Cx46 mRNA expression. ** $P < 0.01$.

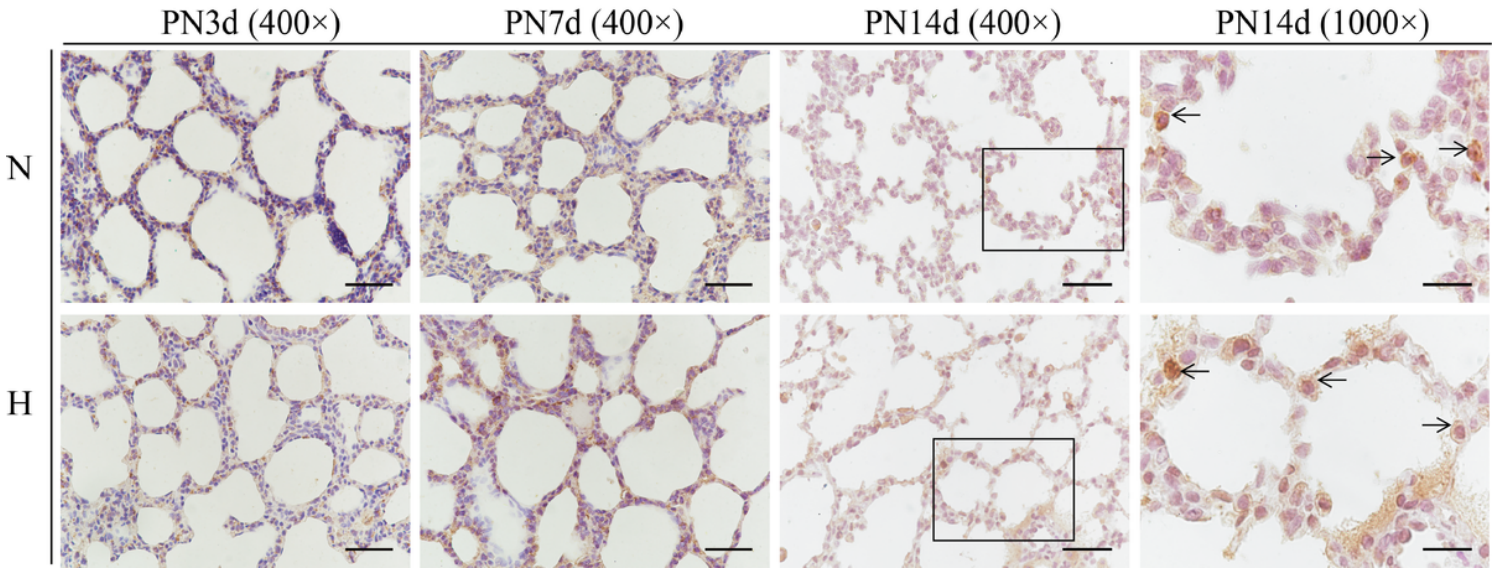

Figure 5

The immunohistochemical staining of Cx26 in lung tissue of neonatal rats (400 × Scale 50 μ m one thousand × Scale 12.5 μ m)

Cx26: connexin 26; N: Normoxia group; H: Hyperoxia group; PN3d: 3 days after birth; PN7d: 7 days after birth; PN14d: 14 days after birth. The area within the black frame of PN14d is observed with a 1000x oil lens.

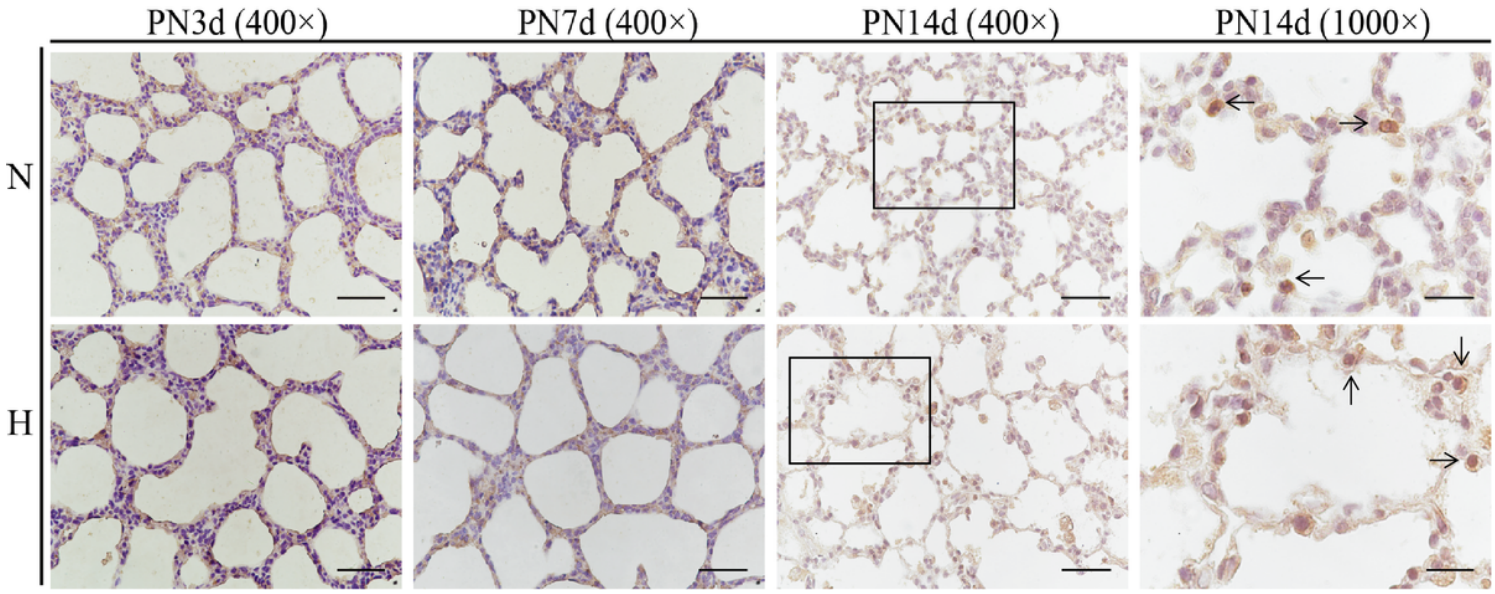

Figure 6

The immunohistochemical staining of Cx32 in lung tissue of neonatal rats (400 × Scale 50 μ m one thousand × Scale 12.5 μ m)

Cx32: connexin 32; N: Normoxia group; H: Hyperoxia group; PN3d: 3 days after birth; PN7d: 7 days after birth; PN14d: 14 days after birth. The area within the black frame of PN14d is observed with a 1000x oil lens.

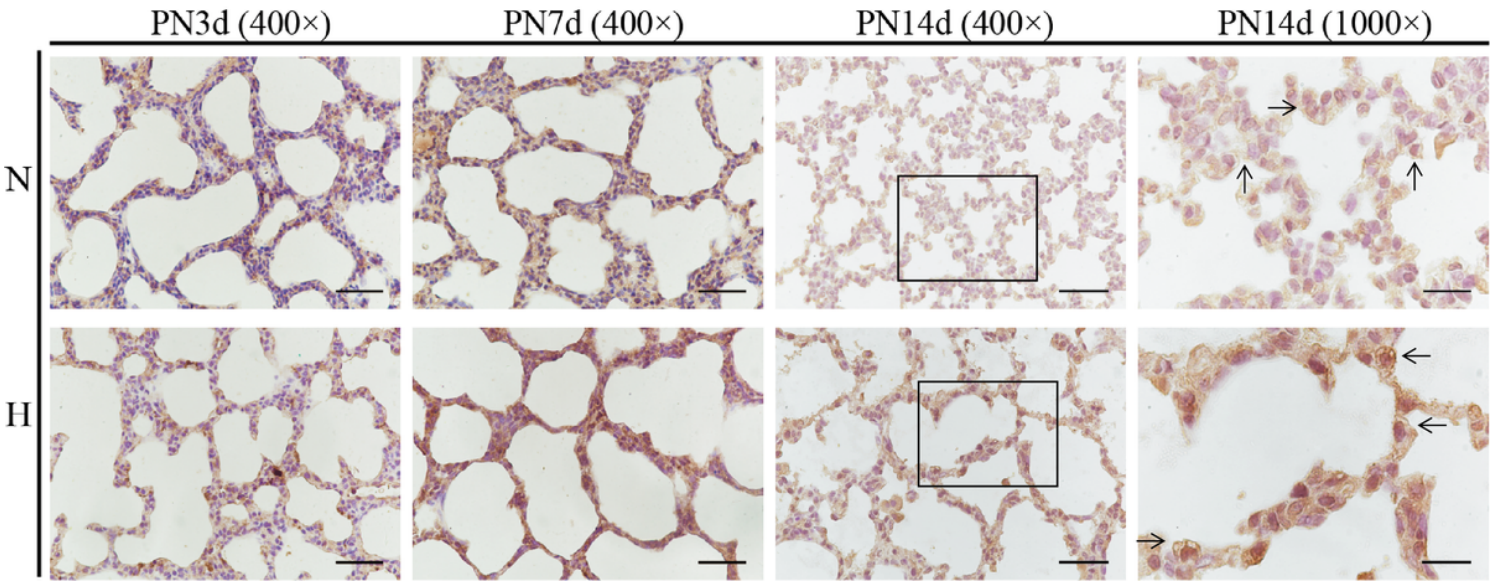

Figure 7

The immunohistochemical staining of Cx43 in lung tissue of neonatal rats (400 × Scale 50 μ m one thousand × Scale 12.5 μ m)

Cx43: connexin 43; N: Normoxia group; H: Hyperoxia group; PN3d: 3 days after birth; PN7d: 7 days after birth; PN14d: 14 days after birth. The area within the black frame of PN14d is observed with a 1000x oil lens.

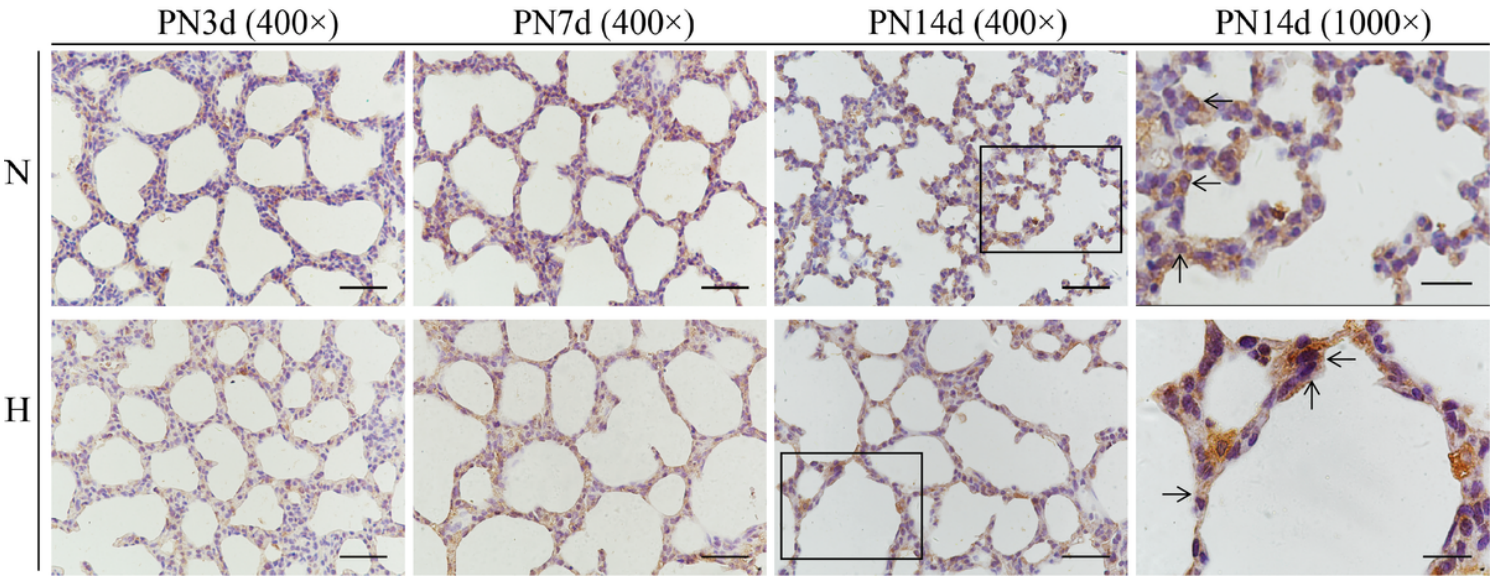

Figure 8

The immunohistochemical staining of Cx46 in lung tissue of neonatal rats (400 × Scale 50 μ m one thousand × Scale 12.5 μ m)

Cx46: connexin 46; N: Normoxia group; H: Hyperoxia group; PN3d: 3 days after birth; PN7d: 7 days after birth; PN14d: 14 days after birth. The area within the black frame of PN14d is observed with a 1000x oil lens.

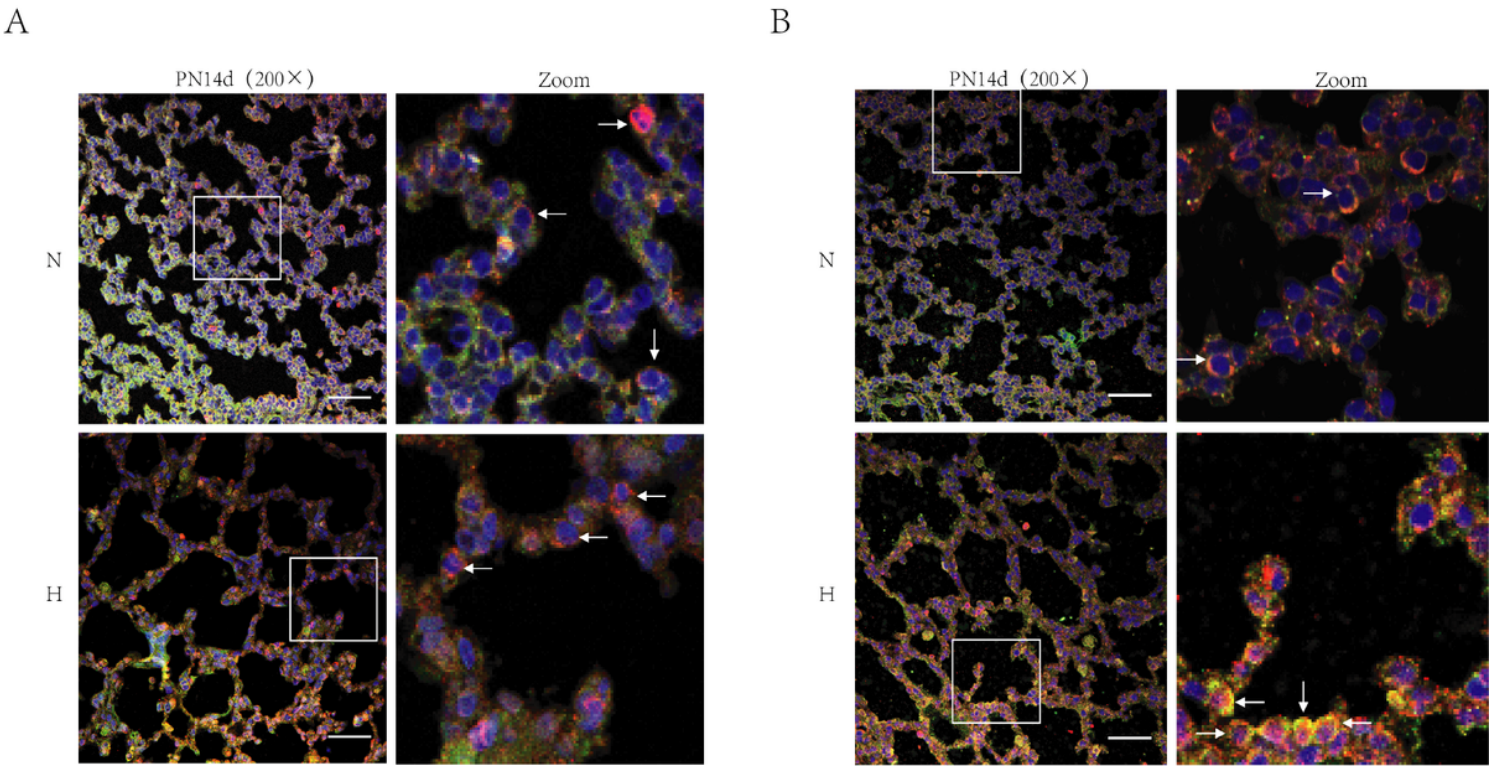

Figure 9

The expression of Cx26 in alveolar epithelial cells (200 × Scale 100 μ m

A: The expression of Cx26 in ATI cells. Red fluorescence represents Cx26 expression, green fluorescence-labeled AQP5 represents ATI cells, and double stained cells appear orange representing the expression of Cx26 in the ATI cells. B: The expression of Cx26 in ATII cells. Red fluorescence represents Cx26 expression, green fluorescence-labeled P180 represents ATII cells, and double stained cells appear orange representing the expression of Cx26 in the ATII cells.. Zoom is the enlargement of the white box image in the left picture. N: Normoxia group; H: Hyperoxia group.

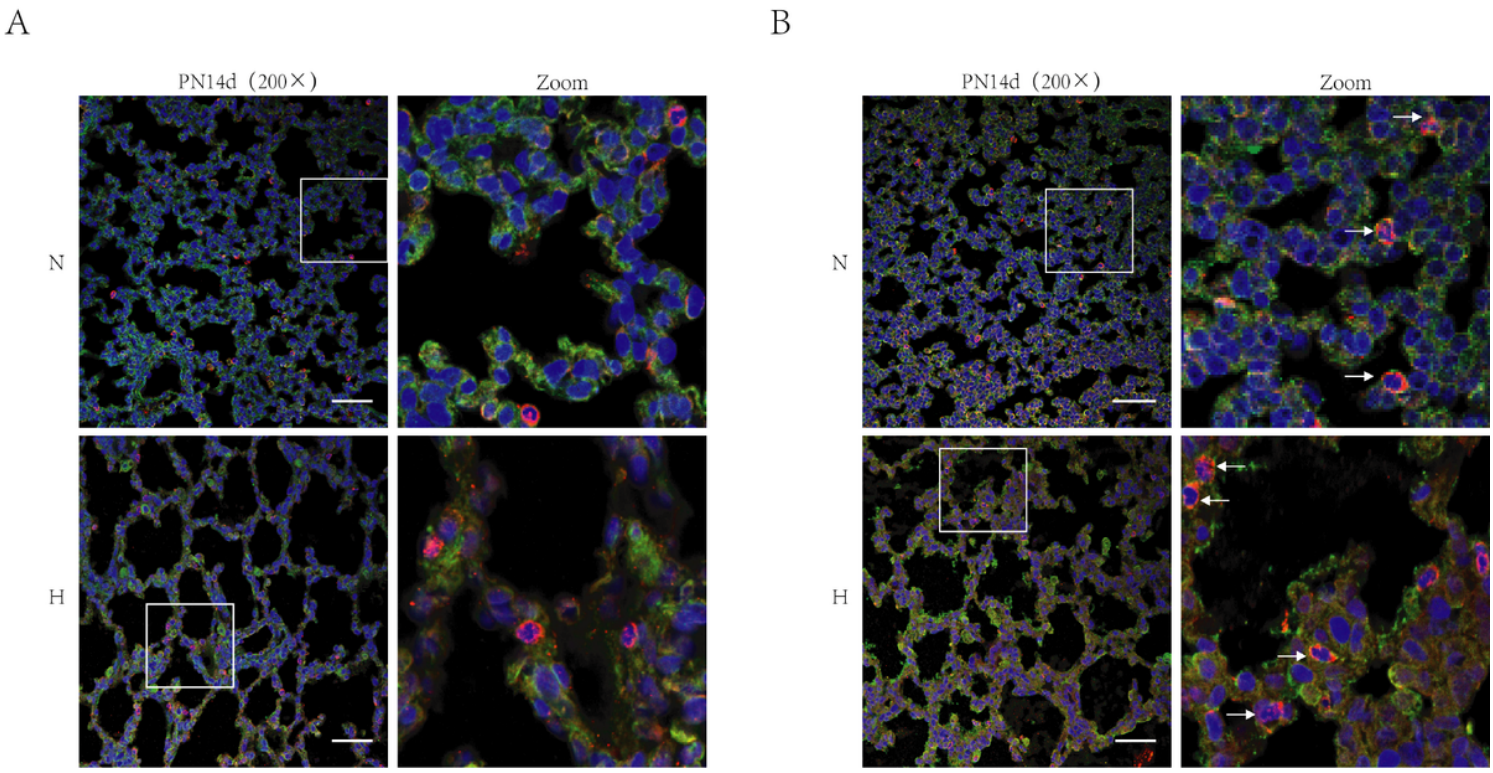

Figure 10

The expression of Cx32 in alveolar epithelial cells (200 × Scale 100 μ m

A: The expression of Cx32 in ATI cells. Red fluorescence represents Cx32 expression, green fluorescence-labeled AQP5 represents ATI cells, and double stained cells appear orange representing the expression of Cx32 in the ATI cells. B: The expression of Cx32 in ATII cells. Red fluorescence represents Cx32 expression, green fluorescence-labeled P180 represents ATII cells, and double stained cells appear orange representing the expression of Cx32 in the ATII cells.. Zoom is the enlargement of the white box image in the left picture. N: Normoxia group; H: Hyperoxia group.

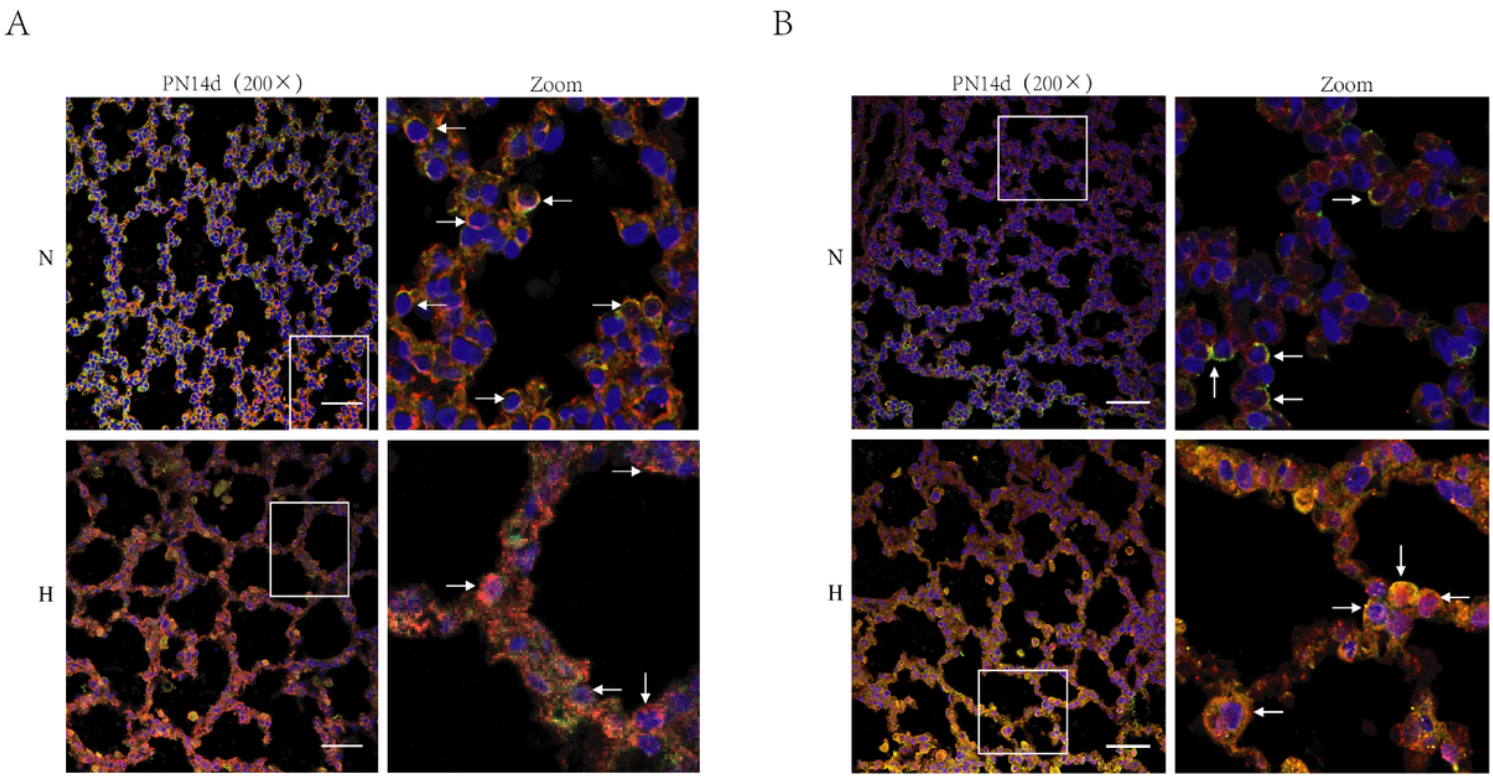

Figure 11

The expression of Cx43 in alveolar epithelial cells (200 × Scale 100 μ m

A: The expression of Cx43 in ATI cells. Red fluorescence represents Cx43 expression, green fluorescence-labeled AQP5 represents ATI cells, and double stained cells appear orange representing the expression of Cx43 in the ATI cells. B: The expression of Cx43 in ATII cells. Red fluorescence represents Cx43 expression, green fluorescence-labeled P180 represents ATII cells, and double stained cells appear orange representing the expression of Cx43 in the ATII cells.. Zoom is the enlargement of the white box image in the left picture. N: Normoxia group; H: Hyperoxia group.

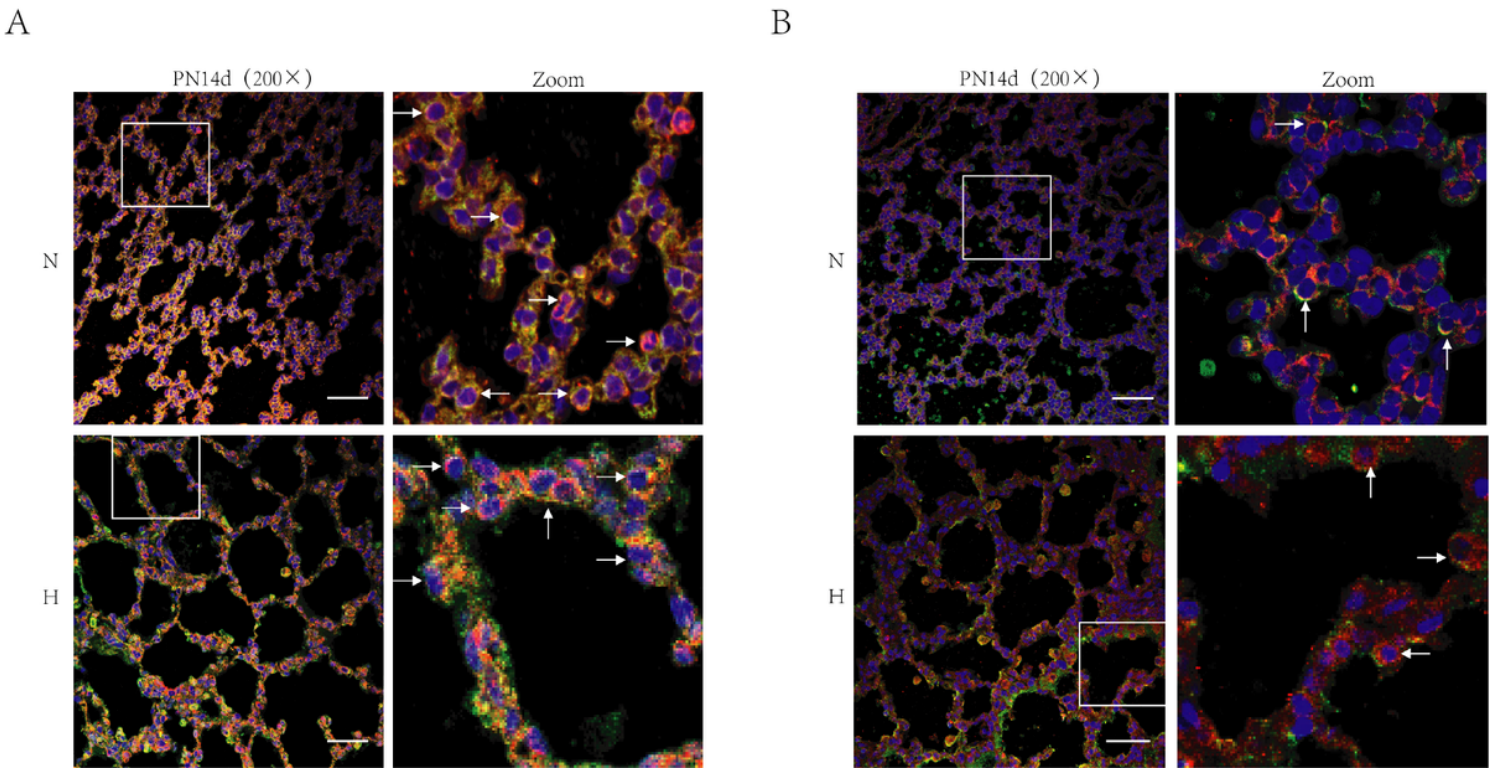

Figure 12

The expression of Cx46 in alveolar epithelial cells (200 × Scale 100 μ m

A: The expression of Cx46 in ATI cells. Red fluorescence represents Cx46 expression, green fluorescence-labeled AQP5 represents ATI cells, and double stained cells appear orange representing the expression of Cx46 in the ATI cells. B: The expression of Cx46 in ATII cells. Red fluorescence represents Cx46 expression, green fluorescence-labeled P180 represents ATII cells, and double stained cells appear orange representing the expression of Cx46 in the ATII cells.. Zoom is the enlargement of the white box image in the left picture. N: Normoxia group; H: Hyperoxia group.

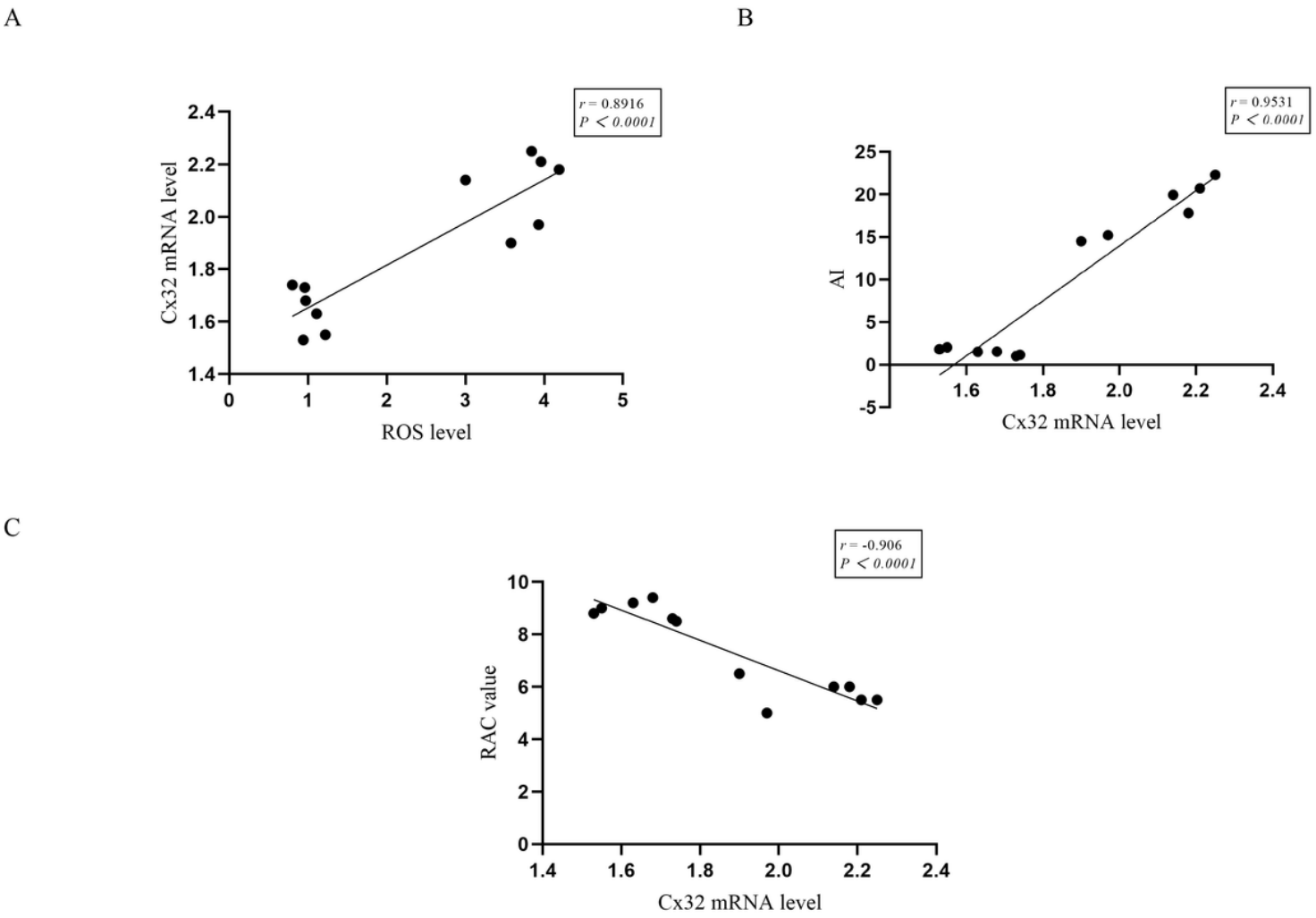

Figure 13

The correlation analysis between Cx32 mRNA level and ROS level, apoptosis index (AI) and RAC value in lung tissue of newborn rats.

A: Cx32 mRNA level was positively correlated with ROS level ($P < 0.0001$). B: C32 mRNA level was positively correlated with AI ($P < 0.0001$). C: Cx32 mRNA level was negatively correlated with RAC value ($P < 0.0001$).